Molecular Dynamics Simulations of Polyplexes and Lipoplexes Employed in Gene Delivery

Deniz Meneksedag-Erol, Chongbo Sun, Tian Tang and Hasan Uludag

Abstract Gene therapy is an important therapeutic strategy in the treatment of a wide range of genetic disorders. Delivery of genetic materials into patient cells is limited since nucleic acids are vulnerable to degradation in extra- and intra-cellular environments. Design of delivery vehicles can overcome these limitations. Polymers and lipids are effective non-viral nucleic acid carriers; they can form stable complexes with nucleic acids known as polyplexes and lipoplexes. Despite the great amount of experimental work pursued on polymer or lipid based gene delivery systems, detailed atomic level information is needed for a better understanding of the roles the polymers and lipids play during delivery. This chapter will review molecular dynamics simulations performed on polyplexes and lipoplexes at critical stages of gene delivery. Interactions between various carriers and nucleic acids during the formation of polyplexes/lipoplexes, condensation and aggregation of nucleic acids facilitated by the carriers, binding of the polyplexes/lipoplexes to cell membrane, as well as their intracellular pathway are reviewed; and the gaps in the theoretical field are highlighted.

Keywords Molecular dynamics · Gene delivery · Non-viral carriers · Polyplex · Lipoplex · Plasmid DNA · siRNA

D. Meneksedag-Erol · H. Uludag (✉)
Department of Biomedical Engineering, Faculty of Medicine and Dentistry and Engineering, University of Alberta, Edmonton, AB, Canada
e-mail: huludag@ualberta.ca

C. Sun · T. Tang
Department of Mechanical Engineering, Faculty of Engineering, University of Alberta, Edmonton, AB, Canada

H. Uludag
Department of Chemical and Materials Engineering, Faculty of Engineering, University of Alberta, Edmonton, AB, Canada

H. Uludag
Faculty of Pharmacy and Pharmaceutical Sciences, University of Alberta, Edmonton, AB, Canada

A. Prokop et al. (eds.), *Intracellular Delivery II*, Fundamental Biomedical Technologies 7, DOI: 10.1007/978-94-017-8896-0_15,

Abbreviations

RNAi	RNA interference
dsRNA	Double stranded RNA
RISC	RNA-induced silencing complex
siRNA	Short interfering RNA
DOPC	1,2-Dioleoyl-sn-glycero-3-phosphocholine
DOPE	Dioleoylphosphatidylethanolamine
DOTAP	1,2-Dioleoyl-3-trimethylammonium-propane
DMTAP	Dimyristoyltrimethylammonium propane
DMPC	Dimyristoylphosphatidylcholine
DPPC	Dipalmitoylphosphatidylcholine
PAMAM	Polyamidoamine
PBAE	Poly(beta-amino ester)
PEI	Polyethylenimine
PLL	Poly-L-lysine
CDP	Cyclodextrin-polycation
CME	Clathrin-mediated endocytosis
CvME	Caveolae/raft-mediated endocytosis
EGF	Epidermal growth factor
MD	Molecular dynamics
MM	Molecular mechanics
QM	Quantum mechanics
PME	Particle mesh Ewald
PBC	Periodic boundary conditions
DPD	Dissipative particle dynamics
US	Umbrella sampling
WHAM	Weighted histogram analysis method
DFT	Density functional theory
CG	Coarse-graining
PTI	Pancreatic trypsin inhibitor
ENM	Elastic network model
LJ	Lennard-Jones
MM-PBSA	Molecular mechanic/Poisson–Boltzmann surface area
DAP	1,3-Diaminopropane
DAPMA	*N*,*N*-Di-(3-aminopropyl)-*N*-(methyl)amine
TAP	Trimethylammonium
MC	Monte Carlo
PMF	Potential of mean force
CA	Caprylic acid
LA	Linoleic acid

1 Background on DNA and siRNA Delivery Systems

Gene therapy aims to modify expression of genes or correct abnormal genes by delivering genetic material into specific patient cells for treatment of wide range of genetic disorders, including cancer, inflammatory, metabolic, infectious cardiovascular and neurological diseases (Pack et al. 2005; Zhang et al. 2012). In gene-based therapy of cancers, targeting tumour suppressor pathways has been an attractive approach since the first clinical trial of p53 gene replacement for treatment of non-small lung carcinoma in 1996 (McNeish et al. 2004; Roth et al. 1996). Since then, 64 % of gene therapy trials have been focused on treatment of cancer diseases (J Gene Med 2013). The initial impetus behind gene therapy has been the desire to use functional DNA-based expression vectors (be in viral or non-viral form) to synthesize therapeutic proteins in situ. This approach relies on the delivery of exogenous DNA cassettes so as to tap into the local cellular protein synthesis machinery. The DNA in this case need to be cellularly internalized, trafficked to the nucleus and recruit the appropriate transcription factors for production of mRNAs for desired proteins. Such proteins have been intended for local activity, where the proteins are functional at the vicinity of the gene delivery site, as well as systemically, where the locally produced proteins are distributed throughout the organism to function systemically. With the discovery of RNA interference (RNAi) mechanism involving double stranded RNAs (dsRNAs) (Fire et al. 1998), the scope of gene therapy was expanded by relying on RNAi-based therapies (Zhang et al. 2012). RNAi is a post-transcriptional gene silencing process triggered by dsRNA molecules in animals and plants. Relatively long dsRNA molecules are cleaved by the enzyme Dicer, which belongs to Ribonuclease III family, into short RNA molecules, which are 21–22 nucleotides in length (Dominska and Dykxhoorn 2010; Elbashir et al. 2001). These dsRNA molecules consist of a passenger and a guide strand, which need to be dissociated into single strands to incorporate into RNA-induced silencing complex (RISC) via guide strand (Matranga et al. 2005). Passenger strand is released after entry into RISC and guide strand direct RISC to complementary sequence in target mRNAs, resulting in mRNA cleavage and gene silencing (Dominska and Dykxhoorn 2010). The practical (therapeutic) use of RNAi relies on short ($\sim$22 nucleotide pairs) synthetic dsRNAs intended to undertake silencing for a pharmacological effect and are named short interfering RNAs (siRNAs). siRNAs could be further chemically modified (e.g., conjugated with cholesterol) for improved delivery and/or pharmacological effect (Lorenz et al. 2004).

The great interest in deploying DNA and siRNA based gene therapeutics has been dampened to some degree due to many challenges encountered in the delivery of the agents and design of effective and safe gene therapy systems.

1.1 Complexation with Carrier Vectors and Condensation

While the first step in therapeutic delivery of DNA and RNA based nucleic acid reagents is systemic administration and extracellular penetration to target sites, we will consider cellular entry as the first step in delivery for the purposes of this manuscript. Significant limitations exist that prevent naked nucleic acids to be efficiently delivered into cells. The negatively charged and hydrophilic nucleic acids are not efficient to cross hydrophobic and negatively charged lipid bilayers of cell membranes (Zhang et al. 2012). Physical strategies that allow delivery of naked nucleic acids into cells, such as electroporation (Potter 1988), gene gun (Fynan et al. 1993) and ultrasound (Yoon and Park 2010), have been developed; but naked nucleic acids can lose their functionality in cells due to their vulnerability to cellular enzymes, ultimately leading to degradation by nucleases. This limitation stimulated the design of delivery systems in which nucleic acids are complexed and protected by delivery vehicles or carriers. Early attempts to design efficient delivery systems concentrated on viral vectors, since viruses are able to effectively transfer their genetic code to host cells. However, with the risk of high immunogenic responses, use of synthetic, non-viral carriers has garnered interest, which can provide a safer and effective alternative. Nucleic acids complexed with cationic polymers and lipids are referred to as 'polyplexes' and 'lipoplexes', respectively (Guo et al. 2010). Common examples of effective synthetic carriers include (1) cationic lipids such as 1,2-dioleoyl-sn-glycero-3-phosphocholine (DOPC), dioleoylphosphatidylethanolamine (DOPE), 1,2-dioleoyl-3-trimethylammonium-propane (DOTAP), dimyristoyltrimethylammonium propane (DMTAP), dimyristoylphosphatidylcholine (DMPC), dipalmitoylphosphatidylcholine (DPPC), and (2) cationic polymers such as polyamidoamine (PAMAM), poly(beta-amino ester) (PBAE), polyethylenimine (PEI), poly-L-lysine (PLL) and cyclodextrin-polycation (CDP) [reviewed in (Aliabadi et al. 2012)]. These carriers are able to bind to nucleic acids via electrostatic interactions between cationic moieties on carriers and anionic phosphate groups of nucleic acids, and condense (or aggregate) the nucleic acids into nanoparticles capable of being protected from degradation and their cellular uptake facilitated (Kircheis et al. 2001).

1.2 Interactions with Cell Membrane and Cellular Uptake

Cell surface binding of nucleic acid polyplexes and lipoplexes is triggered by ionic interactions between cationic carriers and anionic membrane proteins and/or anionic cell-surface 'receptors' such as heparan sulfates and integrins (Aliabadi et al. 2012; Elouahabi and Ruysschaert 2005; Zhang et al. 2012). After an effective cell surface binding, polyplexes and lipoplexes are internalized by endocytosis via a variety of mechanisms such as clathrin- and caveolin-1 independent, clathrin-mediated (CME), caveolae/raft-mediated (CvME) and macropinocytosis (Hillaireau and

Couvreur 2009). The individual mechanisms follow specific intercellular trafficking pathways that may affect the functionality of polyplexes and lipoplexes (Aliabadi et al. 2012). Carriers can also be designed in order to target specific cell types and ligands, such as asialoglycoprotein, epidermal growth factor (EGF), folate, integrin, lactose, mannose, and transferrin (Zhang et al. 2012). Many factors influence the uptake mechanism, such as the cargo (siRNA or DNA) and nature of carrier, the ligand targeted, and its intracellular trafficking pathway. Some studies suggested the CvME to be most conducive to transfection of complexes, while other studies suggested the CME to be the most efficient mechanism. Macropinocytosis was also proposed to be the most efficient mechanism in the transfection of complexes, in particular for larger size complexes that are not ideal for CvME and CME based mechanisms. These contradictory observations complicate identifying the optimal mechanism that polyplexes and lipoplexes follow in their cellular uptake and show the dependency of a functional effect on complex size and nature, as well as the cell types targeted for delivery (Hsu and Uludag 2012).

1.3 Intracellular Trafficking and Cytoplasmic Release

Upon endocytosis, intracellular trafficking of polyplexes/lipoplexes begins in early endosomes. Early endosomes generally fuse into late endosomes (pH $\sim$ 5–6) and transfer their content to lysosomes that have an acidic environment with pH as low as $\sim$4.5. Lipoplexes and polyplexes trapped in these acidic environments must efficiently escape into cytosol in order for the cargo not to be degraded and to reach its target (i.e., nucleus in the case of DNA and mRNA/RISC locations in cytoplasm in the case of siRNA) (Aliabadi et al. 2012; Dominska and Dykxhoorn 2010; Elouahabi and Ruysschaert 2005; Pack et al. 2005; Zhang et al. 2012). It is possible to enhance the endosomal escape of polyplexes/lipoplexes based on the use of fusogenic lipids and proteins, pH sensitive carriers, and photosensitive agents (Dominska and Dykxhoorn 2010). In the case of complexes with certain cationic polymers, such as PEI, endosomal escape is possible through the 'proton-sponge effect' (Boussif et al. 1995); protonation of secondary and tertiary amines of carriers in the low pH environment prevents further acidification, leading to swelling of PEI/nucleic acid particles due to increase in their radius of gyration. The influx of counterions into endosomes also follows to balance the H^+ concentration between the lysosomal compartment and cytoplasm. The resulting osmotic swelling of lysosomal compartment releases the complexes and other contents into the cytoplasm (Boussif et al. 1995; Dominska and Dykxhoorn 2010).

After the nucleic acids are released into cytoplasm, polyplexes/lipoplexes must be dissociated in order for the nucleic acids to be functional. Anionic endogenous molecules such as cytoplasmic RNA (mRNA, tRNA, miRNA, etc.) and glycosaminoglaycans such as heparin sulfate are thought to be involved in dissociation mechanism of lipoplexes and polyplexes (Moret et al. 2001). Electrostatic

interactions between nucleic acids and polymeric carriers are thought to be weakened during the endosomal escape stage due to swelling and pH changes, hence facilitating the release of the nucleic acids from complexes (Aliabadi et al. 2012). After the release, the plasmid DNA (pDNA) has to reach nucleus for transcription and siRNA needs to incorporate into RISC and initiate mRNA cleavage for gene silencing. However naked nucleic acids also face cytoplasmic challenges on their way to pursue their functions since susceptibility to nucleases and cleaving agents may interfere with the pathway on their route and make them non-functional.

1.4 Application of Molecular Dynamics Simulations to Nucleic Acid Delivery

Despite the intensive experimental work on polymer and lipid based gene carriers, many issues related to their mechanisms of action cannot be directly addressed from experiments due to the lack of experimental tools at atomic resolution. Molecular dynamics (MD) is a simulation technique where intra- and intermolecular interactions are described by potential energy functions defined in empirical force fields, motion of atoms are obtained through the integration of equations of motion, and physical properties can be extracted via time average of the equilibrated systems. Since the introduction of the first simulation on a biological macromolecule in 1977 (McCammon et al. 1977), MD simulation has become a very useful tool in analyzing complex biological systems, and there has been an increasing interest in applying these simulations with the recent advances in computational methods and capability.

Recently, there has been a great amount of work pursued on MD simulations of gene delivery systems, and they shed light on many important interactions involved in the delivery pathway. On the complexation of nucleic acids with carrier vectors, MD simulations have provided insight into the mechanisms, dynamics and energetics of binding and complex formation, as well as how they are affected by the molecular composition and structure of the carrier vectors. On the uptake of complexes by cells, complementing the vast experimental work using imaging techniques, MD simulations have been run to study the translocation of delivery systems through lipid bilayers. These simulations have revealed residues that are responsible for interaction with cell membrane, thereby pointing some directions in how to enhance cellular attachment and penetration. On the intracellular behavior of the delivered nucleic acid complexes, with the help of MD simulations, the effects of pH and electrostatic interactions on endosomal escape are now better understood. Despite these existing works, there is still an urgent need for additional simulations to study many other aspects of nucleic acid delivery such as the dissociation of nucleic acids from the polyplexes and lipoplexes.

In the following sections of this manuscript, an introduction to the MD method and different simulation techniques will be first given, followed by a detailed

review on the simulations performed to date on polyplexes and lipoplexes. Future perspectives will be provided on how MD simulations can further assist in our understanding and designing of effective polymer and lipid based gene carriers.

2 Molecular Dynamics Simulations

2.1 Fundamental Principles of Molecular Simulations

MD is a useful computational methodology for generating detailed atomistic information such as atomic coordinates and velocities in a system. The microscopic information of a system is connected to its macroscopic properties through the theoretical framework of 'statistical mechanics'. Statistical mechanics began with the studies by Maxwell and Boltzmann in late 1800s on the kinetic theory of gases. At the end of 19th century, Gibbs introduced a generalized formulation, statistical ensemble theory, which enabled the derivation of macroscopic thermodynamic properties from microscopic mechanical properties (Patria and Beale 2011). Classical mechanics constituted the basis of Gibbs' statistical ensemble theory since it was developed before the evolution of quantum mechanics.

To demonstrate the basic idea of statistical mechanics, let us consider a system constituted by N particles. The microscopic state of the system at time t can be described by a set of $6N$ quantities, namely the positions and momenta of the N particles $(\mathbf{q}_1(t), \ldots, \mathbf{q}_N(t), \mathbf{p}_1(t), \ldots, \mathbf{p}_N(t))$, where the vectors $\mathbf{q}_i(t)$and $\mathbf{p}_i(t)$ represent the position and momentum of particle i, respectively. These $6N$ quantities generate a multi-dimensional space called '*phase space*' with $6N$ axes (Tuckerman 2010; Wereszczynski and McCammon 2012). Any point in the phase space is called a phase point and it represents a microstate of the system. The total energy of the system written in terms of the particles' positions and momenta is the Hamiltonian:

$$\mathcal{H}(\mathbf{q}_1, \ldots, \mathbf{q}_N, \mathbf{p}_1, \ldots, \mathbf{p}_N) = \sum_{i=1}^{N} \frac{\mathbf{p}_i^2}{2m_i} + U(\mathbf{q}_1, \ldots, \mathbf{q}_N) \tag{1}$$

where the first term is the summation of the particles' kinetic energy, m_i being the mass of particle i, and the second term is the system's potential energy, usually as a function of the particles' positions. By knowing the Hamiltonian of the system, the equations of motion can be obtained in terms of the derivatives of the Hamiltonian, and they form a set of $6N$ first order differential equations:

$$\frac{d\mathbf{q}_i}{dt} = \frac{\partial \mathcal{H}}{\partial \mathbf{p}_i} = \frac{\mathbf{p}_i}{m_i}; \quad \frac{d\mathbf{p}_i}{dt} = -\frac{\partial \mathcal{H}}{\partial \mathbf{q}_i} = -\frac{\partial U}{\partial \mathbf{q}_i} = \mathbf{F}_i(\mathbf{q}_1, \ldots, \mathbf{q}_N) \tag{2}$$

where $\mathbf{F}_i(\mathbf{q}_1, \ldots, \mathbf{q}_N)$ is the force acting on particle i. Time trajectory of a phase point can be obtained by integrating Eq. (2) with given initial conditions so that time evolution of the system can be monitored (Tuckerman 2010).

To relate the microstates of the system to its macroscopic state, it is necessary to introduce the concept of *ensemble*. An ensemble is a collection of points in the phase space that correspond to different microstates but share the same macroscopic state defined by measurable thermodynamic parameters such as pressure (P), temperature (T), volume (V), total mass (M) or total number of particles (N). There exist different ensembles in which different thermodynamic parameters are held fixed. In a *microcanonical ensemble*, which represents an isolated system, the macroscopic state of the system is given by a fixed number of particles N, a fixed volume V and a fixed amount of internal energy E. This ensemble is therefore also referred to as an NVE ensemble. The microcanonical ensemble is highly hypothetical, since it is difficult to find a truly isolated system in reality. As a result, other ensembles are defined to account for situations where the internal energy can vary. Commonly used ensembles include the *canonical ensemble*, which corresponds to a constant number of particles N, a constant volume V and a constant temperature T (NVT ensemble); the *isothermal-isobaric ensemble*, which has a fixed number of particles N, a fixed pressure P and a fixed temperature T (NPT ensemble, close to typical experimental conditions); and *grand canonical ensemble*, where the fixed macroscopic parameters are chemical potential μ, volume V and temperature T (μVT ensemble). Grand canonical ensemble is particularly useful to describe systems involving addition or removal of particles, such as in the cases of liquid-vapor equilibrium, capillary condensation etc. (Tuckerman 2010).

At thermodynamic equilibrium, each ensemble has a specific probability distribution $\rho(\mathbf{q}_1, \ldots, \mathbf{q}_N, \mathbf{p}_1, \ldots, \mathbf{p}_N)$ for the microstates. The *ensemble average* of a quantity $A(\mathbf{q}_1, \ldots, \mathbf{q}_N, \mathbf{p}_1, \ldots, \mathbf{p}_N)$ can be calculated from the probability distribution (Leach 2001; Salinas 2001):

$$\langle A \rangle = \frac{\int A(\mathbf{q}_1, \ldots, \mathbf{q}_N, \mathbf{p}_1, \ldots, \mathbf{p}_N)\rho(\mathbf{q}_1, \ldots, \mathbf{q}_N, \mathbf{p}_1, \ldots, \mathbf{p}_N)d\mathbf{q}_1, \ldots, d\mathbf{q}_N d\mathbf{p}_1, \ldots, d\mathbf{p}_N}{\int \rho(\mathbf{q}_1, \ldots, \mathbf{q}_N, \mathbf{p}_1, \ldots, \mathbf{p}_N)d\mathbf{q}_1, \ldots, d\mathbf{q}_N d\mathbf{p}_1, \ldots, d\mathbf{p}_N}. \quad (3)$$

The denominator in Eq. (3) is related to the so-called *partition function*, Z, by a non-dimensionalization factor. Partition function is one of the most important quantities in statistical mechanics. Given the type of ensemble, it essentially captures the number of accessible microscopic states in the phase space. Theoretically, once the partition function is known, all macroscopic thermodynamic quantities such as entropy, enthalpy and free energy can be determined from it (Tuckerman 2010). Practically, however, analytical calculation of the partition function is only possible for a few very simple systems. In addition, direct numerical computation of the partition function is extremely difficult due to the 6N-dimensional integration involved in its definition. In MD simulations,

properties of the simulated system are determined from *time averages* (Eq. 4) over a period τ:

$$A_{avg} = \lim_{\tau \to \infty} \frac{1}{\tau} \int_{t=0}^{\tau} A(\mathbf{q}_1(t), \ldots, \mathbf{q}_N(t), \mathbf{p}_1(t), \ldots, \mathbf{p}_N(t))dt \tag{4}$$

The *Ergodic hypothesis* assumes that the time average (Eq. 4) is equivalent to the ensemble average (Eq. 3), which allows for the use of MD to evaluate macroscopic properties of the system from the motion of the atoms (Szasz 1996).

2.2 Classical Approach: All-Atom Molecular Dynamics

Classical approach to atomistic simulations is based on molecular mechanics (MM), where atoms as treated as soft balls and bonds as elastic sticks (Meller 2001). The intra- and intermolecular interactions in the simulated system is described by a *force field*, in which a mathematical expression of the potential energy is given in terms of geometrical variables such as atom distances and bond angles. The force acting on each atom is calculated from the negative gradient of potential energy function specified in the force field. Numerical integration of equations of motion from this force leads to time trajectory of the system (González 2011). MM and the development of force fields are associated with several approximations, such as the pair-wise additivity of the potential energy. These approximations were introduced in order to simplify the modeling of molecules in MD simulations; since predicting detailed atomistic structures from quantum mechanical (QM) approaches is computationally very expensive. The first force fields, systematic force fields, were developed by Shneior Lifson, Harold Scheraga and Norman Allinger in 1960s, while the most popular ones that are being used today for biomolecules, CHARMM (Brooks et al. 1983) and AMBER (Pearlman et al. 1995) were developed in 1980s (Monticelli and Tieleman 2013; Schlick 2010).

Time trajectory of a system in a classical MD simulation is generated by integrating the Newtonian equations of motion for every atom i:

$$\mathbf{a}_i = \frac{d^2\mathbf{q}_i}{dt^2} = \frac{\mathbf{F}_i}{m_i}, \tag{5}$$

where $\mathbf{a}_i$ is the acceleration of atom i. Given the initial coordinates $(\mathbf{q}_1(0), \ldots, \mathbf{q}_N(0))$ and velocities $\left(\frac{d\mathbf{q}_i}{dt}(0), \ldots, \frac{d\mathbf{q}_N}{dt}(0)\right)$ of all atoms in the system, Eq. (5) can be integrated. However, because the interparticle forces are nonlinear functions of positions, the integration needs to be done numerically. There are several integration algorithms for solving such equations, such as Verlet (Verlet 1967), velocity Verlet

(Swope et al. 1982), Leap-frog (Buneman 1967; Hockney 1970) and Beeman (Schofield 1973) algorithms. The choice of integration method depends on its applicability to the given system (Tuckerman 2010) and the required accuracy. In a typical MD simulation, at each time step, the forces acting on the atoms are calculated from the force field and the current positions of the atoms. Coordinates and velocities are solved and updated using the specified integration algorithm. Energy is calculated and averaged, and written as an output along with the new coordinates. Such a step is repeated until the desired simulation time is reached (Lindahl 2008).

Computationally the most costly part of an MD simulation is the calculation of forces. The computation of electrostatic interactions is particularly time-consuming due to the long-ranged nature of the Coulombic interactions. Several techniques have been developed in order to expedite the calculation of electrostatic forces, such as Ewald summation, lattice summation and fast multipole methods (Sagui and Darden 1999). Particle Mesh Ewald (PME) (Darden et al. 1993) is one of the Ewald summation methods, and is one of the most widely used methods for treating electrostatics. The PME method is based on creating a three-dimensional grid over the system, mapping the atomic charges onto the grid, and separating the summation of electrostatic interactions into a short-ranged part that converges quickly in real space and a long-ranged part that converges quickly in Fourier space. The use of the PME method requires the application of periodic boundary conditions (PBC), through which the system is made infinite-like by having exact replicas of the original system throughout a lattice. Along with PBC, PME has been shown to result in physically stable systems and accurate prediction of long range electrostatics (Phillips et al. 2005).

By solving Eq. (5), the MD simulation is implicitly run in a microcanonical ensemble. This is because the forces are calculated from the negative gradient of the potential energy function, which means that these are conservative forces, and hence the total energy of the system is fixed. To realize MD simulations for other ensembles, special techniques need to be introduced to hold other quantities, such as pressure and temperature, constant. To this end, many thermostats (to maintain constant temperature) and barostats (to maintain constant pressure) have been developed. Examples of thermostats include velocity re-scaling, Berendsen (Berendsen et al. 1984), Andersen (Andersen 1980), Nosé-Hoover (Hoover 1985; Nosé 1984), Langevin dynamics (Schneider and Stoll 1978) and dissipative particle dynamics (DPD) (Hoogerbrugge and Koelman 1992). For barostats, Berendsen (Berendsen et al. 1984) and Nosé-Hoover (Hoover 1985; Nosé 1984) are the most commonly used techniques (Tuckerman 2010).

In an MD simulation, some atoms may have high frequency motions that require very small time steps in the integration, hence slowing down the simulation. One way to increase the time efficiency is to allow larger time steps by constraining some intramolecular interactions, such as bond lengths and angles, thus preventing motions with very high frequency. There are several algorithms developed for this purpose; mostly used ones are SHAKE (Ryckaert et al. 1977), which is based on Verlet integration algorithm and used for constraining positions,

and RATTLE (Andersen 1983), which is based on velocity Verlet algorithm and used for constraining both positions and velocities (Schlick 2010). Constraints/restraints in MD simulations can also be applied when the system has the high likelihood of being trapped in free energy wells, resulting in poor sampling. The umbrella sampling (US) method (Torrie and Valleau 1977) is one such example, in which a biasing potential is applied to restrain certain degrees of freedom of the molecules. To obtain sufficient sampling, a series of simulations are generally needed in US with different biasing potential applied in each simulation. The results are then unbiased and combined for analysis via statistical approaches such as the weighted histogram analysis method (WHAM) (Kumar et al. 1992).

Classical all-atom MD simulations provide all the detailed atomistic information regarding the system of interest: structural information such as molecular size (radius of gyration, etc.), molecular spacing, conformational changes (folding, bending, etc.), hydrogen bond forming and breaking; energetic information such as cohesion energy and free energy of binding. Certainly, the use of all-atom MD is limited by the time and length scales that can be handled within a practical period of time. The current state-of-the-art all-atom MD simulations can simulate less than a million atoms for less than one microsecond, which is typically much smaller compared with practical systems studied in experiments. Another challenge associated with all-atom MD is the accuracy of the force fields employed in these simulations (Lyubartsev et al. 2009; Schlick 2010). Nevertheless, with the fast growing computing power, great efforts on improving numerical efficiency, and extensive studies being conducted on developing advanced, more reliable force fields, these simulations demonstrate immense potential towards modeling systems of realistic time and length scales.

2.3 Hybrid Approach: QM/MM Simulations

Combination of QM approach with MM is originated from the need of compromise between maintaining a reasonable size of the simulated system and accurately describing the electronic structure for certain chemically active regions in the system. While MM is incapable of capturing the changes in electronic structures in these regions such as charge transfer or excitation of electrons, it is possible to take them into account via calculations at the QM level. On the other hand, QM computation for the entire domain of a large molecular system is not feasible, and the QM transformations often happen in a much smaller subset of the system. This motivated the creation of hybrid system models (QM/MM) in which the chemically active region is modeled with QM approach, while the surrounding environment is modeled with classical MM approach. Since the introduction of this approach by Warshel and Levitt in (Warshel and Levitt 1976), QM/MM method has been widely applied to simulation of biomolecular systems such as enzymatic systems (Senn and Thiel 2007). As well, a lot of research has been and is being performed at a fundamental level to improve the QM/MM methodology.

In QM/MM calculations, the system of interest is divided into two subsystems: a reactive part that has a small number of atoms to be described by QM and the rest of the system to be described by a force field (MM). For the QM part, *ab initio*, density functional theory (DFT), and semi-empirical approaches are typically used; while the MM part can be modeled with classical force fields such as CHARMM (Brooks et al. 1983), AMBER (Pearlman et al. 1995) and GROMOS (Scott et al. 1999; Monard and Merz 1999). To enable a QM/MM calculation, it is necessary to define an effective Hamiltonian that contains a potential energy function for the system. This potential energy function needs to properly describe the interactions within the QM region, within the MM region, as well as on the QM and MM interface. The last is the most challenging part in QM/MM modeling, as the interactions between QM and MM regions cannot be described at either QM or MM level alone. There have been several approaches for approximating the interactions between these two levels, and they are mainly categorized into two groups, namely subtractive coupling and additive coupling schemes (Groenhof 2013).

In subtractive coupling, the potential energy of the system, including both QM and MM regions, is first calculated at MM level ($U_{MM}(QM + MM)$). Then the potential energy of the QM region is calculated at QM level ($U_{QM}(QM)$) and added to $U_{MM}(QM + MM)$. Finally, the potential energy of the QM region is calculated at MM level ($U_{MM}(QM)$) and subtracted, i.e.,

$$U_{QM/MM} = U_{MM}(QM + MM) + U_{QM}(QM) - U_{MM}(QM) \tag{6}$$

The implementation of subtractive scheme is straightforward without the need to explicitly connect the QM and MM parts. However, to determine $U_{MM}(QM)$, a force field is required for the QM region and it should be adaptive to chemical changes (e.g., bond breaking or formation) occurring in that region, which is unlikely to be available in most cases (Groenhof 2013).

In additive coupling, the potential energy of the system is calculated by the summation of three terms: QM level energy of the QM region ($U_{QM}(QM)$), MM level energy of the MM region ($U_{MM}(MM)$) and QM-MM energy for the interactions between the two regions ($U_{QM-MM}(QM + MM)$):

$$U_{QM/MM} = U_{QM}(QM) + U_{MM}(MM) + U_{QM-MM}(QM + MM) \tag{7}$$

For this approach, most efforts have been spent on developing methods to evaluate $U_{QM-MM}(QM + MM)$, which explicitly defines the interactions between the QM and MM regions. Commonly used approaches include; for example mechanical embedding where the interactions between the QM and MM regions are treated with force field models, electrostatic embedding which improves mechanical embedding by adding polarization effects, and polarization embedding which provides further improvement on the treatment of polarization effects using several methods such as charge-on-a-spring (Lamoureux and Roux 2003), induced

dipole (Warshel et al. 2006) and fluctuating charge models (Rappe and Goddard 1991), (Groenhof 2013).

Once the potential energy and hence the effective Hamiltonian of the QM/MM system is defined, it will allow the determination of wave function, energy and forces in the system, and an MD simulation can be run. As in classical MD, structural and energetic information can be obtained by unrestrained or restrained simulations. In addition, QM/MM simulations allow the investigation of electronic changes and chemical reactions in the system, which is not possible with classical MD. For example, the reaction pathway can be determined by generating the potential energy surface; the chemical reactivity of a system can be evaluated by calculating the free energy difference between reactants and product. Despite these advantages, the time scale for QM/MM simulations has been limited by the high computational cost of the QM calculations. While one can perform MD for hundreds of nanoseconds, QM/MM simulations can only be performed for hundreds of picoseconds at ab initio or DFT levels, although this can be extended 100 times with the application of semi-empirical approaches. Considering such limitations, most of the QM/MM simulations performed so far have focused on structural optimization (energy minimization) rather than unrestrained dynamics (Groenhof 2013).

2.4 Mesoscopic Approach: Coarse-Grained Simulations

To overcome the computational limits associated with classical MD simulations, there has been a great effort to develop novel approaches that has the ability to bridge atomistic and mesoscopic scales. Coarse-grained (CG) method represents one of such modeling approaches. The first CG model was proposed by Levitt and Warshel in (Levitt and Warshel 1975) for bovine pancreatic trypsin inhibitor (PTI). Since then many different CG models have been developed and applied to study protein folding, protein-protein interactions, membrane proteins, lipid bilayers, complex nucleic acids, nanocomposites, to name a few (Ingólfsson et al. 2013; Takada 2012).

In CG, instead of modeling every atom separately as in all-atom MD, a certain number of atoms are clustered into beads, namely CG sites (Voth 2009). The process of building a CG model consists of several important steps. The first step is to decide the resolution of the model, i.e., how many atoms will be clustered into one bead. In the second step, the location of the CG sites and their arrangement should be determined, with each CG site representing a relatively rigid region in the molecule. Afterwards, the interactions among the CG sites need to be described, and this is often done via parameterized effective potential energy functions, as in the all-atom MD simulations. For example, bonded interactions are generally described by elastic network models (ENM) and Lennard-Jones (LJ) like potentials can be used to model short-ranged non-bonded interactions. Parameterization of these potential energy functions can be achieved using a number of

different approaches (e.g. force-matching, inverse Boltzmann fitting, etc.) in order to produce good agreement between the CG model and experimental data or higher level (QM, MM) calculations (Saunders and Voth 2013).

When the CG model for a system of interest is developed, CG simulations can be performed in a similar manner to that of classical MD simulations. Besides pure CG simulations, CG approach is often coupled with all-atom simulations to connect the information at atomistic and mesoscopic scales. Several methods facilitate building of such connection, including free energy method which determines key interactions from CG simulations and performs more accurate free energy calculation at atomistic scale, inverse mapping method which uses CG simulations to identify regions of the phase space not easily sampled by all-atom MD and allows additional MD simulations in these regions, and multiple-scale approach where the entire system is separated into MM and CG domains in a way similar to QM/MM simulations (Saunders and Voth 2013; Schlick 2010).

The greatest advantage of CG method is the reduction in the degrees of freedom of the systems, leading to larger length and time scales that can be simulated. While time scales are limited to ps in QM/MM and ns in all-atom MD, one can perform CG simulations in the ms range. As a result, direct comparison may be made with experimental observables (Voth 2009). It should be recognized, however, that treating several atoms as a group in CG models causes the loss of atomistic scale information, and can lead to inaccuracy for the data obtained from the simulation trajectories (Takada 2012). Careful evaluation of the quality of the CG model and the method of the simulation should be carried out when employing the CG approach.

3 Molecular Dynamics Simulations on the Formation of Polyplexes and Lipoplexes

In this section, we will provide a detailed review of simulations reported on the formation of polyplexes and lipoplexes. A list of the studies we included in the review is given in Table 1. The structures of the carriers reviewed in the scope of this manuscript are given in Fig. 1.

3.1 Complexation of Polymers or Lipids to Individual Nucleic Acids

All-atom and CG simulations have been used as efficient tools, respectively at atomistic and mesoscopic levels, in analyzing nucleic acid interactions with carriers, such as lipids, polyamines and polymers. A significant amount of efforts have been spent on understanding how the carriers bind and complex with individual

Table 1 Summary of studies on formation of polyplexes and lipoplexes

Interacting molecule	Investigated phenomena	Biomolecule simulated	Type of simulation	References
(a) Binding of carriers to nucleic acids				
Polyamines	DNA-polyamine interactions	dsDNA	All-atom MD	Korolev et al. (2001, 2002, 2003, 2004a, b)
Triazine dendrimers	Effect of dendrimer flexibility and DNA/siRNA comparison	dsDNA, siRNA	All-atom MD	Pavan et al. (2010c)
Spermine, DAP, DAPMA dendrons	Effect of dendrimer generation	dsDNA	All-atom MD	Jones et al. (2010)
Spermine dendrons	Effects of dendrimer flexibility and salt addition	dsDNA	All-atom MD	Pavan et al. (2009)
	Effect of dendrimer structural modification and DNA/siRNA comparison	dsDNA	All-atom MD	Pavan et al. (2010a, b)
	Effect of dendrimer structural modification	dsDNA	CG DPD	Posocco et al. (2010)
PAMAM	Effect of dendrimer flexibility	siRNA	All-atom MD	Jensen et al. (2010, 2011), Pavan et al. (2010a)
	Effects of dendrimer generation and DNA sequence on binding	ssDNA	All-atom MD	Maiti and Bagchi (2006)
	Effects of dendrimer generation, salt and H_2O on binding	dsDNA	All-atom MD	Nandy and Maiti (2011)
	Effect of dendrimer generation and binding of multiple dendrimers	siRNA	All-atom MD	Ouyang et al. (2010a, b), Vasumathi and Maiti (2010)
	Effect of dendrimer protonation ratio	siRNA	All-atom MD	Ouyang et al. (2011), Pavan et al. (2010d)
	Effects of dendrimer generation and protonation ratio	siRNA	All-atom MD	Karatasos et al. (2012)
	Effect of H_2O on binding	dsDNA	US MD	Mills et al. (2013)
PLL	Effect of dendrimer generation and binding of multiple dendrimers	siRNA	All-atom MD	Ouyang et al. (2010b)
	Interactions between DNA and PLL	dsDNA	All-atom MD	Ziebarth and Wang (2009)
	Effect of PLL architecture	dsDNA	All-atom MD	Elder et al. (2011)

(continued)

Table 1 (continued)

Interacting molecule	Investigated phenomena	Biomolecule simulated	Type of simulation	References
PEI	Interactions between DNA and PEI	dsDNA	All-atom MD	Ziebarth and Wang (2009)
	Effect of molecular weight, structure and protonation ratio	dsDNA	All-atom MD	Sun et al. (2011b, 2012a)
	Interactions with PEI and DNA/siRNA comparison	dsDNA, siRNA	All-atom MD	Zheng et al. (2012)
DMTAP, DMPC	Bilayer interactions	dsDNA	All-atom MD	Bandyopadhyay et al. (1999)
DMPC	Monolayer interactions	dsDNA	All-atom MD	Braun et al. (2003)
(b) Nucleic Acid Condensation				
Counterions	Valence effects	Polyanion	CG MD	Stevens (2001)
Polycation	Effects of number of polycations and charges	Polyanion	CG MC	Dias et al. (2003)
Copolymer chains	Effect of copolymer length and charge ratio	Polyanion	CG MD	Ziebarth and Wang (2010)
PAMAM	Effect of applied force	dsDNA	All-atom MD	Mills et al. (2010)
Polyanion + Fe(III)	Effect of Fe(III)	Polycation	CG MC	Jorge et al. (2012)
(c) Nucleic Acid Aggregation				
NaCl, KCl	Effect of Na^+ and K^+	2 dsDNAs	All-atom MD	Savelyev and Papoian (2007)
Polyamines	Effect of valence	2 dsDNAs	US MD	Dai et al. (2008)
PEI	Effect of PEI protonation ratio and charge ratio	2 dsDNAs	US MD	Bagai et al. (2013)
	Aggregation mechanism	Multiple dsDNAs	All-atom MD	Sun et al. (2011a)
	Effect of PEI lipid substitution	Multiple dsDNAs	All-atom MD	Sun et al. (2012b)
		Multiple siRNAs	All-atom MD	Sun et al. (2013)
Cationic lipids	Self-assembly into bilayer	dsDNA	CG MC	Farago et al. (2006)
Cationic and neutral lipids	Phase transition of packed DNA	dsDNA	CG MD	Farago and Gronbech-Jensen (2009)
DOPE, DOTAP	Phase transition of packed DNA	dsDNA	CG MD	Corsi et al. (2010)
Polycation	Interactions between oppositely charged polyions	Polyanion	CG MC	Hayashi et al. (2002, 2003, 2004)

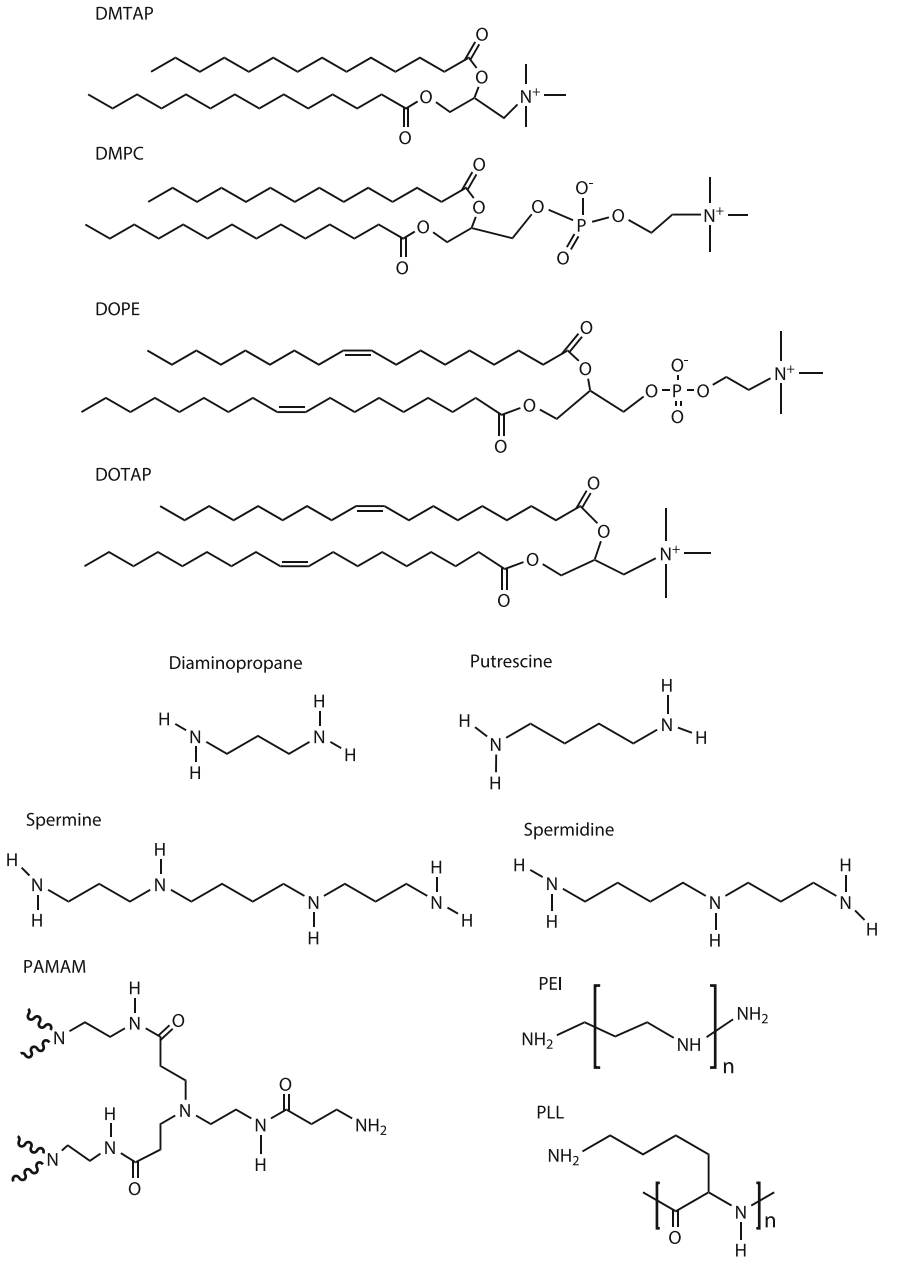

Fig. 1 Chemical structures of selected carriers

nucleic acids, and how the complexation is affected by carrier properties and the environment of complexation. Different types of carriers have been studied, as reviewed below.

3.1.1 Oligocations

Putrescine, spermidine and spermine are small organic oligocations which are naturally present in prokaryotic and eukaryotic cells (Pegg and McCann 1982). They were proposed to bind and stabilize DNA (Gosule and Schellman 1978); spermine and spermidine were reported to cause DNA or RNA precipitation in solution while putrescine lacks this ability (Razin and Rozansky 1959). DNA-oligocation interactions were investigated by Korolev et al. (2001, 2002, 2003, 2004a, b) in a series of MD studies. Interactions between DNA and putrescine (2^+), spermidine (3^+), spermine (4^+) and synthetic diaminopropane (2^+) were studied in the presence of H_2O and monovalent ions, Na^+ and Cl^-. These oligoamines were found to bind to DNA through their interaction with backbone O1P and O2P atoms. While the tri- and tetravalent spermidine and spermine were excluded from the major groove, the divalent oligoamines putrescine and diaminopropane were found in DNA major groove. Oligocations and Na^+ showed different roles in affecting the hydration of DNA. While Na^+ was reported to organize and attract H_2O in hydration of DNA, oligoamines were observed to repel H_2O from the hydration shell. This observation could be important in the interactions of nucleic acids with carriers in the presence of physiological ion composition.

3.1.2 Dendrimers and Dendrons

Many researchers have recently focused on dendrimers and dendrons, branched structures with repetitive units, as nucleic acid carriers due to their well-controlled chemical architecture. The influences of such parameters as generation number, backbone flexibility, protonation state and functionalization, on the complexation of dendrimers and dendrons with nucleic acids, have been widely investigated.

The effect of protonation was addressed by studying different dendrimer protonations corresponding to different pH environments (Karatasos et al. 2012; Ouyang et al. 2011; Pavan et al. 2010d). Molecular Mechanic/Poisson–Boltzmann Surface Area (MM-PBSA) analysis showed a more favorable dendrimer-siRNA binding at low pH ($\sim$5) compared to neutral pH ($\sim$7) conditions regardless of the dendrimer generation (Karatasos et al. 2012; Ouyang et al. 2011; Pavan et al. 2010d) and this was attributed to higher protonation ratio of dendrimers at lower pH. These studies also demonstrated that the electrostatic attraction between the cationic dendrimers and anionic nucleic acids played a crucial role in their complexation.

The effect of dendrimer flexibility on complexation was addressed in several studies (Jensen et al. 2010, 2011; Karatasos et al. 2012; Pavan et al. 2010a, c). For

PAMAM dendrimer, its rigidity was reported to increase with the increase in size/generation (Jensen et al. 2010, 2011; Pavan et al. 2010a). Pavan and coworkers studied complexation of G4 to G6 PAMAM dendrimers with siRNA. G4 dendrimer showed high binding affinity due to its flexible structure, while affinity towards siRNA was lost with G6 dendrimer's rigid spherical structure. G7 PAMAM simulations with siRNA also showed a rigid sphere behaviour (Jensen et al. 2010) where a lack of structural rearrangement in G7 dendrimers led to less than an optimal binding mode to siRNA. In a separate study (Jensen et al. 2011), comparison between G1, G4 and G7 PAMAM dendrimers showed that the increased rigidity associated with size increase caused higher entropic cost in binding to siRNA. Using MM-PBSA analysis, the free energy of binding between PAMAM dendrimers and siRNA was evaluated. G4 PAMAM was reported to be the most suitable carrier based on its strongest binding affinity as compared to G1 and G7. Rigidity increased with the increase in size from G4 to G7 and binding was weakened (Jensen et al. 2011). Although the flexibility of dendrimers was reported to contribute positively to complexation in most of the studies, a contradictory report was published by Pavan et al. (2010c). Their intent was to prove 'flexibility favors binding', however their results showed a beneficial effect of dendrimer rigidity. G2 triazine dendrimers designed to be flexible with an ethylene glycol chain resulted in a more compact and rigid structure due to the collapse of the flexible linkers in a salt environment, so that the number of interactions with DNA and siRNA were reduced. However, the rigid dendrimer designed with piperazine rings was found to establish more contacts with nucleic acids (Pavan et al. 2010c).

In many situations, the effects of protonation and flexibility are coupled. For example, G5 dendrimers showed a transition from flexible to rigid structures depending on the pH value (Pavan et al. 2010a), which was caused by different protonation ratios at different pH. The flexibility observed at neutral pH (pH $\sim$ 7.4) was lost with a decrease in pH to 5 or lower. At low pH, increase in dendrimer's cationic charge caused an increase in rigidity thus leading to lower affinity towards siRNA (Pavan et al. 2010a). As greater amount of charges facilitate binding through stronger electrostatic interactions but at the same time can make the dendrimer more rigid, there needs to be a delicate balance between charge and flexibility in order to achieve optimal binding. High generation dendrimers are large in size and weight due to the substitution of more building blocks to the low generation ones. They are more rigid but have more charges compared with low generation ones. While some work reported reduced binding affinity as the generation number increases, others reported that high generation PAMAM dendrimers bound more effectively to single stranded DNA (Maiti and Bagchi 2006), double stranded DNA (Nandy and Maiti 2011), and double stranded siRNA (Karatasos et al. 2012; Ouyang et al. 2010a; Vasumathi and Maiti 2010). Similarly, for 1,3-diaminopropane (DAP), *N*,*N*-di-(3-aminopropyl)-*N*-(methyl)amine (DAPMA) and spermine dendrons, Jones et al. (2010) reported an increase in binding affinity towards double stranded DNA with the increase in generation number. Since the dendrimer rigidity increases with the increase in generation number, this increased binding affinity should be considered

in the context of increased dendrimer rigidity. Lower generations might show higher flexibility, but lack of necessary numbers of positive charges might cause ending up with lower binding affinity. The optimal threshold for the number of positive charges and flexibility should be determined in designing optimal dendrimers as nucleic acid carriers.

Functionalizing dendrimers/dendrons with end-groups can also lead to different binding capability to nucleic acids. Jones et al. (2010) studied the interactions between DNA and G1 and G2 dendrons with the end-groups spermine, DAP and DAPMA. MM-PBSA calculations indicated that enthalpic contribution to binding energy was related to surface charges of the dendron. When the surface is more charged, enthalpic contribution to binding energy became more favorable. As the protonable groups on each ligand in the scaffold is 3, 2 and 1 for spermine, DAPMA and DAP, respectively; spermine dendrons were selected to be the best candidates for DNA binding among both G1 and G2 dendrons based on their highest binding energy due to their largest surface charge. On the other hand, binding affinity of G2 DAPMA to DNA was found to be close to that of G1 and G2 spermine dendrons due to its favorable enthalpic interactions associated with ligand backfolding and DNA bending. In the work of Pavan et al. (2010b), a comparison was made between dendrons functionalized with non-degradable spermine and those functionalized with UV degradable spermine. UV degradable dendrons had the same enthalpic affinity towards DNA as non-degradable ones, but had a smaller entropic cost upon binding. UV modification on the structure with a photolabile linker introduced branches. Due to this branched structure, UV modified dendron could establish more stable interactions with DNA via more uniform vibrations of dendron amines and DNA phosphates, resulting in smaller cost in entropy (Pavan et al. 2010b). Posocco et al. modified spermine functionalized dendrons with hydrophobic cholesterol units in order to trigger self-assembly. They performed DPD simulations, a CG approach in which several atoms are lumped into a bead and the interactions between the beads (named DPD particles) are treated with soft potentials. The force acting on each DPD particle is a sum of conservative, dissipative and stochastic forces. Time trajectory can be obtained by solving Newton's equation of motions as in MD. According to their DPD simulations, self-assembly of first generation cholesterol-modified dendrons resulted in assembled dendrimer structures (due to cholesterol aggregation) that have higher charge density compared to second generation dendrons, thus more effective binding with DNA (Posocco et al. 2010).

Simulations with multiple PAMAMs revealed formation of more compact and stable DNA (Vasumathi and Maiti 2010) and siRNA (Ouyang et al. 2010b) complexes, in comparison to systems containing single dendrimers. When polyplexes become positively charged upon the saturation of nucleic acid charges, excess dendrimers would float around in free form (Ouyang et al. 2010b).

Physiological ions and aqueous environment affect the interactions between nucleic acids and carriers. Pavan et al. studied the effect of NaCl addition on complexation of DNA with spermine-functionalized G1 and G2 dendrimers. Increased salt concentration did not show a remarkable effect on binding affinity of

G2 towards DNA, while interactions with DNA were lost in G1 dendrimer-DNA system (Pavan et al. 2009). When salt was introduced to G5 PAMAM-DNA system, MM-PBSA analysis indicated a decrease in binding affinity due to the screening effect. However, the formed complexes were reported to be still very compact (Nandy and Maiti 2011). The screening effect from counterions therefore seems to become important in the case of small carriers; when the carriers are large enough to maintain strong interactions with nucleic acids; screening becomes negligible on the overall binding behavior. H_2O molecules were known to have an impact on nucleic acid-carrier interactions since they are released from the binding region while complexation occurs. Effect of H_2O molecules on DNA-G3 PAMAM interactions was studied by Mills and coworkers by US MD simulations. The results revealed the importance of H_2O ordering; it was found that H_2O molecules were capable of bridging DNA and dendrimer in highly charged dendrimer system (dendrimer carrying +32 charge in comparison to +16) (Mills et al. 2013). The PAMAM (G3 to G5) itself was reported to undergo swelling in the presence of H_2O molecules as a result of H_2O penetration into their structures, and the degree of penetration was proportional to dendrimer generation (Nandy and Maiti 2011). It is therefore important to simulate properly hydrated carriers for more realistic predictions.

The role of nucleic acid sequence in binding to PAMAM dendrimers was studied by Maiti and Bagchi with atomistic MD simulations. Vibrational density of states analysis showed the binding affinity difference between bases; the following order was found in binding to G4 dendrimer: poly(G) > poly(C) > poly(A) > poly(T) (Maiti and Bagchi 2006). Seeing such a difference after employing pure base sequences should not be surprising; however, whether the same result holds true with statistically mixed sequences (especially for longer nucleic acid chains) remains to be seen. In order to compare carrier binding to DNA and siRNA, Pavan et al. performed MD simulations on 21 bp long DNA (sequence: 5′-TCG AAG TAC TCA GCG TAA GTT-3′; 3′-AGC TTC ATG AGT CGC ATT CAA-5′) and siRNA (5′-UCG AAG UAC UCA GCG UAA G dTdT-3′; 3′-dTdT AGC UUC AUG AGU CGC AUU C-5′). Stronger dendron interactions were formed with the siRNA compared to DNA, due to siRNA's higher flexibility than DNA (Pavan et al. 2010b, c). This observation was concurrent to previous results seen with the PAMAM structures, where the rigidity of the carrier reduced the strength of binding.

3.1.3 Cationic Polymers

Despite the great interest in dendrimeric structures as gene carriers, their buffering capacity could be compromised at times (due to covalent modification of protonable residues in the dendritic core) and this led researchers to seek other types of carriers with superior buffering capacity. PEI is one of the most efficient nucleic acid carriers with high buffering capacity (Boussif et al. 1995). PEI-nucleic acid delivery systems were studied with atomistic simulations by Ziebarth and Wang (2009), our group (Sun et al. 2011b, 2012a) and Zheng et al. (2012). The initial

study of PEI-DNA binding by Ziebarth and Wang (2009) reported the main interactions to be formed between the cationic PEI amines and DNA backbone phosphates. Our group focused on the effect of several PEI properties such as molecular weight, structure, and protonation ratio on PEI complexation with DNA. Sizes of PEIs simulated were 570 Da (Sun et al. 2011b) and 2 kDa (Sun et al. 2012a) with different PEI branching structures. The simulations with 570 Da PEI showed that the degree of branching did not have a significant influence on the binding pattern, while the protonation ratio played a key role. Decrease in protonation ratio resulted in less stable complexes due to the loss of direct H-bonding between PEI and DNA (Sun et al. 2011b). In contrast to 570 Da PEI, simulations with 2 kDa PEI (Sun et al. 2012a) showed very different binding pattern associated with linear and branched PEIs. Linear PEI was found to bind to DNA like cords due to its flexible structure, thus providing good coverage of the DNA surface. Branched PEIs, on the other hand, bound to DNA like beads, utilizing part of the PEI molecule to bind to a DNA molecule and potentially allowing interaction of individual PEIs with multiple DNAs. A better neutralization of DNA charges with 2 kDa PEI as compared to 570 Da PEI was observed. Zheng and coworkers studied a high molecular weight branched PEI (25 kDa) binding with DNA and siRNA. Structural and energetic analysis showed that strong electrostatic interactions were formed between DNA and cationic amines of PEI. While charge neutralization between oppositely charged PEI and DNA groups was apparent at the binding interface, several cationic PEI groups that were not contributing to binding were observed away from the interface. Simulations with one dsDNA (21 bp) and one 25 kDa PEI indicated that a stable DNA polyplex required more than one 25 kDa PEI molecule. Energetic comparison between DNA and siRNA complexation with 25 kDa PEI revealed stronger attraction of polymer to siRNA due to its more flexible structure (Zheng et al. 2012). This observation is in agreement with the previously reported comparison between DNA and siRNA in binding to dendrons (Pavan et al. 2010b, c).

Another polymeric carrier, PLL, was reported to be relatively inefficient in DNA charge neutralization (Ziebarth and Wang 2009) due to its linear structure compared to more densely charged PEI. All-atom MD simulations with different PLL structures probed the effect of PLL architecture on DNA binding mechanism. Comparison between linear PLL (uniform charges along the backbone) and grafted oligolysines (charged side-groups) on a neutral backbone showed less favorable binding of DNA with graft oligolysines, which was attributed to the steric hindrance caused by the hydrophobic backbone in graft architecture (Elder et al. 2011). PLL binding to siRNA was studied by Ouyang et al. (2010a, b) in a series of studies along with PAMAM dendrimers. They studied PLL^{4+} and PLL^{8+} systems that have the same charge as G0 and G1 PAMAM dendrimers, respectively. For the PLL-siRNA systems, the complexation behavior was found to be similar to that of the PAMAM-siRNA systems, suggesting that the electrostatic interactions dominated the binding affinities, rather than the molecular structural details.

3.1.4 Lipids

Cationic and neutral lipids are known for their ability to form complexes with nucleic acids to serve as effective carriers in nucleic acid delivery. A natural lipid structure contains a hydrophilic region, the lipid head group, and a hydrophobic region known as the lipid tail. When exposed to an aqueous environment, lipids self-assemble into a bilayer structure in which the hydrophilic head groups are exposed to water while the hydrophobic tails stay in the center region. DNA-lipid interactions were first studied by Bandyopadhyay and coworkers with computational approaches, where atomistic simulations were performed on a mixture of DMTAP and DMPC lipid bilayers interacting with DNA. Zwitterionic PC head groups were found to approach DNA and compete with cationic trimethylammonium (TAP) moieties in neutralizing the DNA phosphate charges (Bandyopadhyay et al. 1999). Braun et al. performed atomistic simulations on the interaction of a protonated DMPC monolayer with DNA. Although the DNA conserved its double helical structure through the simulation period, base pairing was affected by the interactions between the lipid head groups and DNA backbone phosphates as well as bases (Braun et al. 2003). These atomic level studies revealed the screening of the anionic DNA charges by lipid moieties.

3.2 Condensation and Aggregation

DNA condensation is defined as the dramatic decrease in DNA's volume triggered by packaging inside cellular environment. As an example, T4 bacteriophage's DNA occupies a volume of 4×10^9 nm^3 in solution; when it is packed in T4's head, its volume decreases to 5×10^5 nm^3 (Bloomfield 1996). This packaging in cellular environment can be reproduced in solution by the addition of cationic molecules to DNA. Attraction of multiple nucleic acid molecules to each other with the help of condensing agents such as cationic carriers results in formation of self-assembled (ordered) structures or aggregates (disordered structures). These aggregates could turn into spherical nanoparticles that are approximately 100 nm in diameter under practical conditions (Goula et al. 1998). While DNA condensation by cationic carriers is crucial for cellular uptake of DNA, the delivery of siRNA relies more on formation of aggregates. A number of simulations have been performed to study both condensation and aggregation of nucleic acids.

3.2.1 Condensation

Stevens carried out CG MD simulations on DNA-like polyelectrolytes to probe their condensation by di-, tri- and tetravalent counterions. While divalent counterions did not show any condensation, condensation was achieved with trivalent and tetravalent counterions. These results revealed the important interplay of

enthalpic and entropic contributions to condensation. A valence of at least 3 was found to be required for electrostatics to overpower the entropic interactions and cause condensation (Stevens 2001). Dias et al. studied polyanion/polycation systems by CG Monte-Carlo (MC) simulations. The stochastic MC simulations follow a different algorithm than the deterministic MD methodology. Rather than obtaining a time trajectory of the system by integrating Newton's equations of motion in MD, MC method uses a random number generator to obtain new coordinates and performs trial moves (Schlick 2010). Despite the different underlying algorithms, MC simulations also try to sample the phase space as in MD, and for this reason there have been few MC simulations (mostly at the CG scale) on polyplexes and lipoplexes, which will be presented in this review. With the CG MC approach, condensation and collapse of polyanion chains were observed by increasing numbers of polycations or number of charges carried by each polycation. The systems with polycation/polyanion charge ratio below unity resulted in small polyanion chain deformation, but not in collapse or condensation (Dias et al. 2003). Ziebarth and Wang, using CG MD simulations, investigated polyanion condensation mediated by copolymer chains containing neutral hydrophilic and polycationic parts. Variation in copolymer length affected the condensation; successful condensation of polyanions was achieved with chains longer than 4 cationic blocks (Ziebarth and Wang 2010). In agreement with Dias et al. (2003), polyanion condensation was observed when the charge ratio ≥ 1 and only local bending/folding was seen for charge ratios below the unity (Ziebarth and Wang 2010). A CG MC study on compaction of DNA by PEI and Fe(III) (as a ternary system) was reported by Jorge and coworkers. Fe(III) ions were found to be located in the polyanion (corresponding to DNA) regions that were less occupied by polycation (corresponding to PEI) and they were proposed to induce folding of the polyanion chain (Jorge et al. 2012).

DNA condensation by G3 PAMAM dendrimers has been also studied with US MD simulations by Mills et al. (2010). Simulations were performed with 24 bp dsDNA and G3 PAMAM dendrimer with 32 protonated amine groups. Potential of mean force (PMF) calculations were carried out along a reaction coordinate defined as the center of mass distance between PAMAM and DNA. By taking the derivative of PMF with respect to the reaction coordinate, the interaction forces between DNA and dendrimer were calculated to retrieve the transition between extended (uncondensed) and condensed states. When a large force was applied, uncondensed state was favored; with the decrease in the applied force, DNA collapse (condensed state) was reported to be favorable (Mills et al. 2010).

3.2.2 Aggregation

Several studies focused on DNA aggregation by counterions (Savelyev and Papoian 2007), polyamines (Dai et al. 2008) and polymers (Bagai et al. 2013; Sun et al. 2011a, 2012b). Savelyev and Papoian performed all-atom MD simulations with two DNA molecules in the presence of NaCl and KCl. PMF analysis from US

simulations was performed along a reaction coordinate, which was the center of mass distance between two DNA molecules. DNA repulsion when they approach each other was found to follow a steeper profile in the presence of KCl, which indicated that K^+ screening was less efficient than Na^+ screening for DNA charges (Savelyev and Papoian 2007). Dai and coworkers performed US MD simulations to evaluate the PMF of attraction between two DNAs in the presence of linear oligoamines putrescine (2^+), spermidine (3^+) and spermine (4^+). The results revealed more attraction between two DNA molecules with increasing valence of the oligoamine and the formation of transient ion bridges was observed (Dai et al. 2008). Our group (Bagai et al. 2013) reported attraction of two DNA molecules in the presence of 568 Da PEI with US MD simulations. According to PMF analysis, PEI had better capability of aggregating the DNAs compared with oligoamines, leading to larger depth in the PMF curve. In addition, more compact and stable aggregates were obtained when N/P ratio (ratio of the number of PEI Ns to the number of DNA Ps) of the system or protonation ratio of PEI was increased.

In a series of recent publications (Sun et al. 2011a, 2012b, 2013), we reported PEI mediated aggregation of multiple (>2) DNA and siRNA molecules. In the case of 568 Da PEI, DNA aggregation was facilitated by the formation of polyion bridges between DNA molecules and screening of DNA anionic charges (Sun et al. 2011a). Simulations performed on oleic acid modified PEI (831 Da) showed that the lipid moieties on the PEI can bring an additional mechanism of aggregation, namely, the association of lipid tails (Sun et al. 2012b). We further investigated the effect of lipid substitution on PEI-mediated siRNA aggregation (Sun et al. 2013). Simulations were performed for multiple siRNA molecules in the presence of caprylic acid (CA) and linoleic acid (LA) modified 1,874 Da PEI, as well as native (unmodified) PEI. Comparison among them showed more compact and stable siRNA aggregates in the case of lipid substituted systems (Sun et al. 2013). Also, LA association from different PEIs was found to be more stable than the association among shorter CA. Furthermore, the level of substitution was shown to affect the aggregation. At the level of one lipid substitution per PEI, several PEIs were found to stay in the solution instead of binding to the polyplex. However, when the substitution level was increased to three lipids per PEI, all PEIs could bind to the polyplex (see Fig. 2).

Lipid mediated DNA self-assembly was reported by Farago et al. in a series of publications (Farago and Gronbech-Jensen 2009; Farago et al. 2006; Corsi et al. 2010). CG MC simulations on randomly distributed lipids around DNAs revealed the self-assembly of lipids into a bilayer structure along with DNAs sandwiched between two lipid bilayers (Fig. 3a; Farago et al. 2006). In a further CG study (Farago and Gronbech-Jensen 2009), the self-assembly mechanism was studied with a much larger system by using a 10-fold higher number of lipid molecules (e.g., 800 cationic lipids, 1,600 neutral lipids along with 32 DNA molecules) than in (Farago et al. 2006). Charge density, φ_c, of the cationic and neutral lipid mixture, defined as the percentage of the cationic lipid in the mixture, was varied by changing the number of neutral lipids. An inverted hexagonal phase, in which DNA molecules are packed in cylindrical lipid micelles, was observed at

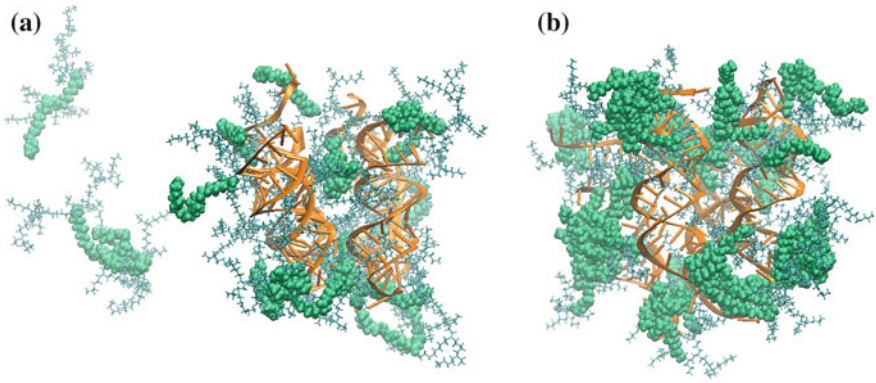

Fig. 2 Formation of polyplex from 4 siRNA and 18 LA-modifed PEI molecules: siRNAs are given in orange, while PEI and LA are *cyan* and *green*, respectively. **a** 1 LA substitution per PEI chain. **b** 3 LA substitution per PEI chain (Sun et al. 2013)

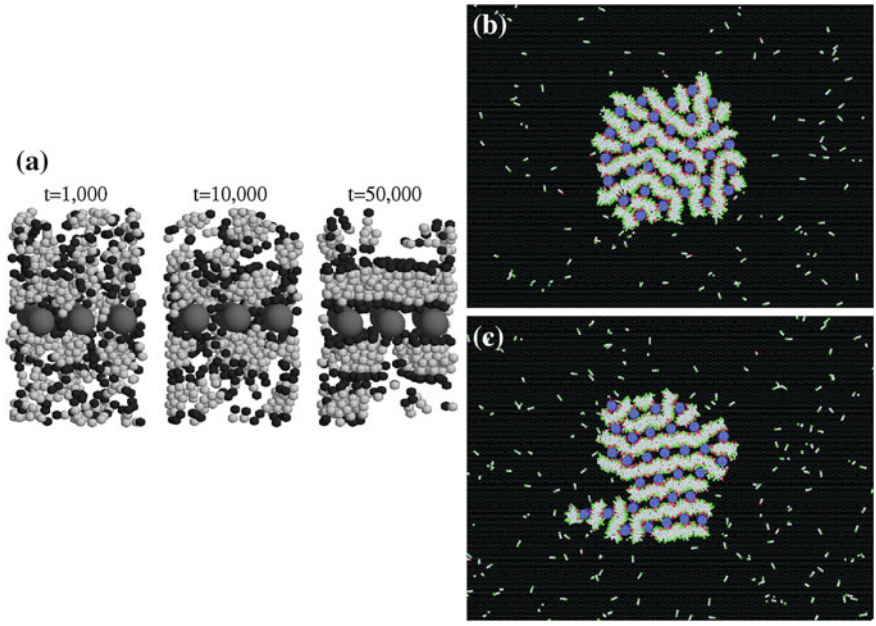

Fig. 3 Snapshots from CG MC simulations on self-assembly of cationic lipids and DNA. The evolution of the system is given in terms of the number of MC steps, t. Hydrophilic and hydrophobic regions of lipids are in *black* and *light gray* respectively, and DNAs are in *dark gray* (Farago et al. 2006). **b** Inverted hexagonal phase, $\kappa_s = 2.5$; and **c** Lamellar phase, $\kappa_s = 5$, of DNA-cationic lipid complexes Adapted with permission from Farago and Gronbech-Jensen (2009). Copyright 2013 American Chemical Society

intermediate charge densities ($4/15 \leq \varphi_c \leq 2/5$). At high charge densities (i.e. in a fully charged system, $\phi_c = 1$), a highly ordered square lattice form was visualized. Further, they modified the stiffness of the membrane by assigning an energy penalty for adjacent lipids to have different orientations. When the stiffness of the membrane increased (e.g. as the stiffness parameter κ_s changed from 2.5 to 5), transition from hexagonally packed DNA structure to a lamellar phase, in which DNA monolayers are sandwiched in between lipid bilayers, was observed (Fig. 3b, c). Increasing κ_s to >5 resulted in formation of lamellar phase only (Farago and Gronbech-Jensen 2009). Corsi et al. (2010) performed CG MD simulations on the assembly of DNA-DOPE and DNA-DOPE-DOTAP systems, where the experimentally observed transition of the DNA-DOPE-DOTAP system from fluid lamellar to inverse hexagonal phase was successfully reproduced. They further studied the phase transition of lipoplexes as a function of hydration level (number of H_2O molecules per lipid). Two H_2O molecules per lipid resulted in transition from lamellar to hexagonally packed DNAs in the presence of DOPE lipids, while addition of DOTAP to the system did not cause remarkable changes at the mesoscopic scale (Corsi et al. 2010).

In addition to the above works that studied particular carrier molecules, investigation of interactions between oppositely charged polyions has been attempted as a model of nucleic acid-carrier systems. Instead of modeling nucleic acid or carrier structures at atomistic level, simplifying nucleic acids as polyanions and cationic carriers as polycations allow researchers to investigate the aggregation mechanism with reduced computational costs. With that motivation, Hayashi et al. (2002, 2003, 2004) employed CG MC simulations on oppositely charged polyions. The effects of polyion's absolute charge, charge density and surrounding salt concentration on the aggregation mechanism were explored. All systems they studied had either 10 cationic polyions (Hayashi et al. 2002, 2003), or 20 cationic polyions (Hayashi et al. 2004) while the number of anionic polyions was varied so as to generate a fully cationic system (no anionic polyions) and systems with charge equivalencies (ratio between number of polyanions and number of polycations) of 20, 50, 90 and 100 % (Hayashi et al. 2002, 2003). Under salt-free conditions, aggregate formation was found to be variable with the increased charge equivalency. While formation of positively charged aggregates was favorable at 50 % charge equivalency, increasing charge equivalency up to 100 % led to the formation of only neutral aggregates. In addition, with 100 % charge equivalency, the formed aggregate tended to be small, i.e., the probability of having an aggregate formed with 1 polycation and 1 polyanion chain (1:1 aggregate) was higher than that of larger aggregates such as 2:2 or 3:3. Addition of salt shortened the Debye length of the solution, thereby reducing the electrostatic attraction between oppositely charged polyions. This led to formation of smaller aggregates (Hayashi et al. 2003). The same tendency was observed by decreasing the absolute charge of the polyions (Hayashi et al. 2004). These observations revealed the important interplay of electrostatic and entropic contributions to aggregate formation. Formation of large aggregates was electrostatically favorable due to the attractive forces, while smaller clusters were promoted to gain translational

entropy (Hayashi et al. 2002, 2003, 2004). Although these CG MC simulations do not involve nucleic acids or carriers, the observed aggregation behavior should be applicable to nucleic acid delivery systems. They provided useful information on how one may better control the sizes of practical nucleic acid/carrier aggregates for delivery in cellular systems.

4 Molecular Dynamics Simulations on the Cell Membrane Interactions and Intracellular Pathway of Polyplexes and Lipoplexes

For internalization, polyplexes/lipoplexes have to go through the first delivery stage, namely the interaction with cell membranes prior to endocytosis. The first molecular level modeling regarding the attachment of dendrimer-DNA polyplexes to cell membranes was introduced by Voulgarakis et al. (2009). CG MC simulations with a G5 dendrimer-DNA complex showed that increasing the negative membrane charge density (reduced charge density in the range of 0 to 10) and decreasing Debye length of solution had a negative effect in cell membrane attachment. Specifically, when the charge density of membrane was increased, dendrimers were shown to dissociate from DNA (Voulgarakis et al. 2009), indicating the destabilizing effect of increasing membrane charge. Decreasing the Debye length had a similar effect on causing the instability of the complexes. These are important parameters that should be taken into consideration when evaluating the efficiency of cell attachment and delivery.

After attachment to cell membrane, the next step is internalization of polyplexes/lipoplexes, mainly by endocytosis. This is triggered by the formation of endosomes via cell membrane folding. The first CG model on endocytosis of DNA-nanovector complexes was introduced by Ding and Ma (2013). The nanovector used in their study consisted of polymer chains, each with protonable polyelectrolytes and representative surface ligands, while the modeled membrane was composed of oppositely charged lipids and receptors. Pre-complexed structures of dsDNA (modeled as rigid rods) and the nanovector were placed on top of the membrane and endocytosis (driven by ligand-receptor interaction) was investigated by varying length and protonation degree of polyelectrolyte, length and concentration of DNA, and membrane charge. Polymers with 1 polyelectrolyte molecule per chain prevented ligand-receptor interactions resulting in partial endocytosis, while those with 3 polyelectrolytes per chain caused full endocytosis. Variation in DNA length and concentration was also found to affect endocytosis. Furthermore, increasing membrane's negative charge resulted in better endocytosis compared to lower charged membranes (Ding and Ma 2013). This study indicated that for a target membrane, optimization of the delivery system (i.e., types of carriers and cargos) should be determined in order to achieve efficient endocytosis.

Following the internalization of polyplexes/lipoplexes is their intracellular pathway after endosomal escape. Although to our knowledge there has not been any atomic level computational work on this topic, Dinh et al. (2007) studied this phenomenon by developing a stochastic simulation model for 25 kDa PEI-DNA polyplexes, where the transition between distinct states, i.e. polyplexes bound to cell membrane, polyplexes inside endosomes, lysosomes, cytoplasm, and unpacked nucleic acids, were investigated. The intracellular pathways of the polyplexes were divided into two categories, namely transport and reaction events. Transport events were the diffusion related events while the reaction events were related to association or dissociation of polyplexes. Parameterization and validation for their computational model was achieved by experiments with the 25 kDa PEI-DNA polyplexes. In the stochastic simulations, they provided cell configurations, constructed based on different cell geometries obtained from experimental imaging techniques, as computational domains. After assigning the computational domains, the change in either cellular environment or polyplexes was updated with a given time step ($\Delta t = 0.2$ s). Transport events were treated by solving equations of motion, while the reaction events were modeled as first-order Markov processes. Ten thousand trajectories were sampled from 200 cells. The effects of several key properties, such as location and time of the endosomal escape, and cell shape on delivery were addressed. On the effect of endosomal escape location, the authors calculated the probability of a successful DNA delivery to nucleus when a polyplex escaped from endosomes at different distances from the nuclear boundary. The results showed the importance of escape location, indicated by 5 % probability of having a successful delivery when the escape occurred in the supranuclear region compared to 1 % probability in the case of an escape into cytoplasm. Further, the impact of escape time (defined as the length of period from transfection to the time when a polyplex escaped from endosomes and entered cytoplasm) was studied by calculating the probability that a polyplex with different escape time could reach the nucleus within 24 h after the escape. With an increase in escape time in the supranuclear region, the probability of reaching nucleus decreased, most likely due to lysosomal degradation. In the cytoplasmic region, the optimum escape time was found to be 12–13 h after transfection. Cell geometry (circularity and size) was also shown to be critical for delivery; greater delivery efficiency was observed when the cells were elongated and smaller. This observation was attributed to the fact that elongated and smaller cells has relatively larger perinuclear space; therefore the escape location is closer to the nucleus in these cells, leading to more efficient delivery (Dinh et al. 2007). Using a computational approach, this study provided clues for optimal conditions for efficient gene delivery to nucleus, which shed light onto the design of optimal delivery systems.

Finally, Jorge et al. investigated the decompaction of polyanion chains (representing DNA), which were pre-compacted by polycations (representing polycationic carriers), in the presence of heparin-like molecules. Heparin is a negatively charged sulfated anticoagulant which is known for its capability to

release nucleic acids from their carrier vectors. Through CG MC simulations, the decompaction of polyanions was shown to be possible with heparin-like molecules, and the extent of decompaction was found to be higher in the presence of both polycations and Fe(III), which might indicate the importance of Fe(III) in facilitating nucleic acid release (Jorge et al. 2012).

5 Future Perspectives

In this chapter, we provided a detailed review on the simulation work performed to-date on the formation of polyplexes and lipoplexes, as well as their intracellular delivery stages. As can be seen from Sect. 3, there has been a great interest towards determining optimal carriers for nucleic acid delivery. Detailed atomic and mesoscopic level data regarding optimal conditions for complexation between various carriers and nucleic acids are beginning to be available in the literature. However, given the low amount of work pursued on the intracellular events in the delivery process, there is an urgent need to fill the gap in theoretical modeling on these crucial stages. All the reviewed works in Sect. 4 involved either mesoscopic or stochastic approaches, and to our knowledge, there has not been any atomic level work due to the significant computational time required for all atom simulations. The lack of atomic level information in mesoscopic approaches may lead inaccuracy in the observed results. With the growing computational power, mesoscopic time scales may be reached by atomistic simulations; thus accurate understanding could be achieved by direct comparison between atomistic trajectories and experimental data.

MD simulations are also providing unique insights into the atomistic structure of polyplexes and lipoplexes, especially with the multifunctional carriers composed of different chemical domains. Our own work has been initially driven by experimental considerations (Hsu and Uludag 2012), but recent theoretical modelling (Sun et al. 2011b, 2012a, b, 2013) is better explaining the outcomes observed in cellular systems. This is critical since it may facilitate the design of next-generation delivery systems based on known experimental and theoretical aspects of current delivery systems. It must be stated that most MD simulations have relied on existing experimental studies for validation and it might be misleading to employ results derived from systems where there is a discrepancy between experimental conditions and theoretical predictions (such as the hydration, salt concentrations, differences in molecular weight of employed species). Conducting simultaneous studies where the experimental and theoretical conditions are harmonized will be beneficial not only for better predictions, but also to improve the theoretical calculations if significant deviations from experimental data are observed.

References

Aliabadi HM, Landry B, Sun C et al (2012) Supramolecular assemblies in functional siRNA delivery: where do we stand? Biomaterials 33:2546–2569

Andersen H (1980) Molecular dynamics simulations at constant pressure and/or temperature. J Chem Phys 72:2384

Andersen HC (1983) Rattle: a "velocity" version of the shake algorithm for molecular dynamics calculations. J Comput Phys 52:24–34

Bagai S, Sun C, Tang T (2013) Potential of mean force of polyethylenimine-mediated DNA attraction. J Phys Chem B 117:49–56

Bandyopadhyay S, Tarek M, Klein ML (1999) Molecular dynamics study of a lipid-DNA complex. J Phys Chem B 103:10075–10080

Berendsen HJC, Postma JPM, van Gunsteren WF et al (1984) Molecular dynamics with coupling to an external bath. J Chem Phys 81:3684

Bloomfield VA (1996) DNA condensation. Curr Opin Struct Biol 6:334–341

Boussif O, Lezoualc'h F, Zanta MA et al (1995) A versatile vector for gene and oligonucleotide transfer into cells in culture and in vivo: polyethylenimine. Proc Natl Acad Sci USA 92:7297–7301

Braun CS, Jas GS, Choosakoonkriang S et al (2003) The structure of DNA within cationic lipid/DNA complexes. Biophys J 84:1114–1123

Brooks BR, Bruccoleri RE, Olafson BD et al (1983) Charmm—a program for macromolecular energy, minimization, and dynamics calculations. J Comput Chem 4:187–217

Buneman O (1967) Time-reversible difference procedures. J Comput Phys 1:517–535

Corsi J, Hawtin RW, Ces O et al (2010) DNA lipoplexes: formation of the inverse hexagonal phase observed by coarse-grained molecular dynamics simulation. Langmuir 26:12119–12125

Dai L, Mu Y, Nordenskiold L et al (2008) Molecular dynamics simulation of multivalent-ion mediated attraction between DNA molecules. Phys Rev Lett 100:118301

Darden T, York D, Pedersen L (1993) Particle mesh Ewald: an N·log(N) method for Ewald sums in large systems. J Chem Phys 98:10089–10092

Dias RS, Pais AACC, Miguel MG et al (2003) Modeling of DNA compaction by polycations. J Chem Phys 119:8150–8157

Ding HM, Ma YQ (2013) Design maps for cellular uptake of gene nanovectors by computer simulation. Biomaterials 34:8401–8407

Dinh AT, Pangarkar C, Theofanous T et al (2007) Understanding intracellular transport processes pertinent to synthetic gene delivery via stochastic simulations and sensitivity analyses. Biophys J 92:831–846

Dominska M, Dykxhoorn DM (2010) Breaking down the barriers: siRNA delivery and endosome escape. J Cell Sci 123(Pt 8):1183–1189

Elbashir SM, Harborth J, Lendeckel W et al (2001) Duplexes of 21-nucleotide RNAs mediate RNA interference in cultured mammalian cells. Nature 411:494–498

Elder RM, Emrick T, Jayaraman A (2011) Understanding the effect of polylysine architecture on DNA binding using molecular dynamics simulations. Biomacromolecules 12:3870–3879

Elouahabi A, Ruysschaert JM (2005) Formation and intracellular trafficking of lipoplexes and polyplexes. Mol Ther 11:336–347

Farago O, Gronbech-Jensen N (2009) Simulation of self-assembly of cationic lipids and DNA into structured complexes. J Am Chem Soc 131:2875–2881

Farago O, Gronbech-Jensen N, Pincus P (2006) Mesoscale computer modeling of lipid-DNA complexes for gene therapy. Phys Rev Lett 96:018102

Fire A, Xu S, Montgomery MK et al (1998) Potent and specific genetic interference by double-stranded RNA in Caenorhabditis elegans. Nature 391:806–811

Fynan EF, Webster RG, Fuller DH et al (1993) DNA vaccines: protective immunizations by parenteral, mucosal, and gene-gun inoculations. Proc Natl Acad Sci USA 90:11478–11482

González MA (2011) Force fields and molecular dynamics simulations. Collect SFN 12:169–200
Gosule LC, Schellman JA (1978) DNA condensation with polyamines I. Spectroscopic studies. J Mol Biol 121:311–326
Goula D, Remy JS, Erbacher P et al (1998) Size, diffusibility and transfection performance of linear PEI/DNA complexes in the mouse central nervous system. Gene Ther 5:712–717
Groenhof G (2013) Introduction to QM/MM simulations. In: Monticelli L, Salonen E (eds) Methods in molecular biology biomolecular simulations: methods and protocols. Springer Science Business Media, New York, pp 43–66
Guo P, Coban O, Snead NM et al (2010) Engineering RNA for targeted siRNA delivery and medical application. Adv Drug Deliv Rev 62:650–666
Hayashi Y, Ullner M, Linse P (2002) A Monte Carlo study of solutions of oppositely charged polyelectrolytes. J Chem Phys 116:6836–6845
Hayashi Y, Ullner M, Linse P (2003) Complex formation in solutions of oppositely charged polyelectrolytes at different polyion compositions and salt content. J Phys Chem B 107:8198–8207
Hayashi Y, Ullner M, Linse P (2004) Oppositely charged polyelectrolytes. Complex formation and effects of chain asymmetry. J Phys Chem B 108:15266–15277
Hillaireau H, Couvreur P (2009) Nanocarriers' entry into the cell: relevance to drug delivery. Cell Mol Life Sci 66:2873–2896
Hockney RW (1970) The potential calculation and some applications. Meth Comput Phys 9:135–211
Hoogerbrugge PJ, Koelman JMVA (1992) Simulating microscopic hydrodynamic phenomena with dissipative particle dynamics. Europhys Lett 19:155
Hoover WG (1985) Canonical dynamics: equilibrium phase-space distributions. Phys Rev A 31(3):1695–1697
Hsu CY, Uludag H (2012) Cellular uptake pathways of lipid-modified cationic polymers in gene delivery to primary cells. Biomaterials 33:7834–7848
Ingólfsson HI, Lopez CA, Uusitalo JJ et al (2013) The power of coarse graining in biomolecular simulations. WIREs Comput Mol Sci
Jensen LB, Mortensen K, Pavan GM et al (2010) Molecular characterization of the interaction between siRNA and PAMAM G7 dendrimers by SAXS, ITC, and molecular dynamics simulations. Biomacromolecules 11:3571–3577
Jensen LB, Pavan GM, Kasimova MR et al (2011) Elucidating the molecular mechanism of PAMAM-siRNA dendriplex self-assembly: effect of dendrimer charge density. Int J Pharm 416:410–418
Jones SP, Pavan GM, Danani A et al (2010) Quantifying the effect of surface ligands on dendron-DNA interactions: insights into multivalency through a combined experimental and theoretical approach. Chemistry 16:4519–4532
Jorge AF, Dias RS, Pais AA (2012) Enhanced condensation and facilitated release of DNA using mixed cationic agents: a combined experimental and Monte Carlo study. Biomacromolecules 13:3151–3161
Journal of Gene Medicine (2013) [cited 2013 May 06]. Available from: www.wiley.co.uk/genmed/clinical
Karatasos K, Posocco P, Laurini E et al (2012) Poly(amidoamine)-based dendrimer/siRNA complexation studied by computer simulations: effects of pH and generation on dendrimer structure and siRNA binding. Macromol Biosci 12:225–240
Kircheis R, Wightman L, Wagner E (2001) Design and gene delivery activity of modified polyethylenimines. Adv Drug Deliv Rev 53:341–358
Korolev N, Lyubartsev AP, Nordenskiold L et al (2001) Spermine: an "invisible" component in the crystals of B-DNA. A grand canonical Monte Carlo and molecular dynamics simulation study. J Mol Biol 308:907–917
Korolev N, Lyubartsev AP, Laaksonen A et al (2002) On the competition between water, sodium ions, and spermine in binding to DNA: a molecular dynamics computer simulation study. Biophys J 82:2860–2875

Korolev N, Lyubartsev AP, Laaksonen A et al (2003) A molecular dynamics simulation study of oriented DNA with polyamine and sodium counterions: diffusion and averaged binding of water and cations. Nucleic Acids Res 31:5971–5981

Korolev N, Lyubartsev AP, Laaksonen A et al (2004a) Molecular dynamics simulation study of oriented polyamine- and Na-DNA: sequence specific interactions and effects on DNA structure. Biopolymers 73:542–555

Korolev N, Lyubartsev AP, Laaksonen A et al (2004b) A molecular dynamics simulation study of polyamine- and sodium-DNA. Interplay between polyamine binding and DNA structure. Eur Biophys J 33:671–682

Kumar S, Rosenberg JM, Bouzida D et al (1992) The weighted histogram analysis method for free-energy calculations on biomolecules. I. The method. J Comput Chem 13:1011–1021

Lamoureux G, Roux B (2003) Modeling induced polarization with classical Drude oscillators: theory and molecular dynamics simulation algorithm. J Chem Phys 119:3025–3039

Leach AR (2001) Molecular modeling principles and applications. Pearson Education Limited, Great Britain

Levitt M, Warshel A (1975) Computer-simulation of protein folding. Nature 253:694–698

Lindahl ER (2008) Molecular dynamic simulations. In: Kukol A (ed) Methods in molecular biology molecular modeling of proteins. Humana Press, pp 3–23

Lorenz C, Hadwiger P, John M et al (2004) Steroid and lipid conjugates of siRNAs to enhance cellular uptake and gene silencing in liver cells. Bioorg Med Chem Lett 14:4975–4977

Lyubartsev A, Tu YQ, Laaksonen A (2009) Hierarchical multiscale modelling scheme from first principles to mesoscale. J Comput Theor Nanosci 6:951–959

Maiti PK, Bagchi B (2006) Structure and dynamics of DNA-dendrimer complexation: role of counterions, water, and base pair sequence. Nano Lett 6:2478–2485

Matranga C, Tomari Y, Shin C et al (2005) Passenger-strand cleavage facilitates assembly of siRNA into Ago2-containing RNAi enzyme complexes. Cell 123:607–620

McCammon JA, Gelin BR, Karplus M (1977) Dynamics of folded proteins. Nature 267:585–590

McNeish IA, Bell SJ, Lemoine NR (2004) Gene therapy progress and prospects: cancer gene therapy using tumour suppressor genes. Gene Ther 11:497–503

Meller J (2001) Molecular dynamics. In: Encyclopedia of life sciences. Nature Publishing Group

Mills M, Orr B, Banaszak Holl MM et al (2010) Microscopic basis for the mesoscopic extensibility of dendrimer-compacted DNA. Biophys J 98:834–842

Mills M, Orr BG, Banaszak Holl MM et al (2013) Attractive hydration forces in DNA-dendrimer interactions on the nanometer scale. J Phys Chem B 117:973–981

Monard G, Merz KM (1999) Combined quantum mechanical/molecular mechanical methodologies applied to biomolecular systems. Acc Chem Res 32:904–911

Monticelli L, Tieleman DP (2013) Force fields for classical molecular dynamics. In: Monticelli L, Salonen E (eds) Methods in molecular biology biomolecular simulations: methods and protocols. Springer Science Business Media, New York, pp 197–213

Moret I, Esteban Peris J, Guillem VM et al (2001) Stability of PEI-DNA and DOTAP-DNA complexes: effect of alkaline pH, heparin and serum. J Control Release 76:169–181

Nandy B, Maiti PK (2011) DNA compaction by a dendrimer. J Phys Chem B 115:217–230

Nosé S (1984) A molecular dynamics method for simulations in the canonical ensemble. Mol Phys 52:255–268

Ouyang D, Zhang H, Herten DP et al (2010a) Structure, dynamics, and energetics of siRNA-cationic vector complexation: a molecular dynamics study. J Phys Chem B 114:9220–9230

Ouyang D, Zhang H, Parekh HS et al (2010b) Structure and dynamics of multiple cationic vectors-siRNA complexation by all-atomic molecular dynamics simulations. J Phys Chem B 114:9231–9237

Ouyang D, Zhang H, Parekh HS et al (2011) The effect of pH on PAMAM dendrimer-siRNA complexation: endosomal considerations as determined by molecular dynamics simulation. Biophys Chem 158:126–133

Pack DW, Hoffman AS, Pun S et al (2005) Design and development of polymers for gene delivery. Nat Rev Drug Discov 4:581–593

Patria RK, Beale PD (2011) Statistical mechanics. Elsevier, United States
Pavan GM, Danani A, Pricl S et al (2009) Modeling the multivalent recognition between dendritic molecules and DNA: understanding how ligand "sacrifice" and screening can enhance binding. J Am Chem Soc 131:9686–9694
Pavan GM, Albertazzi L, Danani A (2010a) Ability to adapt: different generations of PAMAM dendrimers show different behaviors in binding siRNA. J Phys Chem B 114:2667–2675
Pavan GM, Kostiainen MA, Danani A (2010b) Computational approach for understanding the interactions of UV-degradable dendrons with DNA and siRNA. J Phys Chem B 114:5686–5693
Pavan GM, Mintzer MA, Simanek EE et al (2010c) Computational insights into the interactions between DNA and siRNA with "rigid" and "flexible" triazine dendrimers. Biomacromolecules 11:721–730
Pavan GM, Posocco P, Tagliabue A et al (2010d) PAMAM dendrimers for siRNA delivery: computational and experimental insights. Chemistry 16:7781–7795
Pearlman DA, Case DA, Caldwell JW et al (1995) Amber, a package of computer-programs for applying molecular mechanics, normal-mode analysis, molecular-dynamics and free energy calculations to simulate the structural and energetic properties of molecules. Comput Phys Commun 91:1–41
Pegg AE, McCann PP (1982) Polyamine metabolism and function. Am J Physiol 243:C212–C221
Phillips JC, Braun R, Wang W et al (2005) Scalable molecular dynamics with NAMD. J Comput Chem 26:1781–1802
Posocco P, Pricl S, Jones S et al (2010) Less is more—multiscale modelling of self-assembling multivalency and its impact on DNA binding and gene delivery. Chem Sci 1:393–404
Potter H (1988) Electroporation in biology: methods, applications, and instrumentation. Anal Biochem 174:361–373
Rappe AK, Goddard IWA (1991) Charge equilibration for molecular dynamics simulations. J Phys Chem 95:3358–3363
Razin S, Rozansky R (1959) Mechanism of the antibacterial action of spermine. Arch Biochem Biophys 81:36–54
Roth JA, Nguyen D, Lawrence DD et al (1996) Retrovirus-mediated wild-type p53 gene transfer to tumors of patients with lung cancer. Nat Med 2:985–991
Ryckaert JP, Ciccotti G, Berendsen HJC (1977) Numerical integration of the cartesian equations of motion of a system with constraints: molecular dynamics of n-alkanes. J Comput Phys 23:327–341
Sagui C, Darden TA (1999) Molecular dynamics simulations of biomolecules: long-range electrostatic effects. Annu Rev Biophys Biomol Struct 28:155–179
Salinas SRA (2001) Introduction to statistical physics. Springer, New York
Saunders MG, Voth GA (2013) Coarse-graining methods for computational biology. Annu Rev Biophys 42:73–93
Savelyev A, Papoian GA (2007) Inter-DNA electrostatics from explicit solvent molecular dynamics simulations. J Am Chem Soc 129:6060–6061
Schlick T (2010) Molecular modeling and simulation: an interdisciplinary guide. Springer, New York
Schneider T, Stoll E (1978) Molecular-dynamics study of a three-dimensional one-component model for distortive phase transitions. Phys Rev B 17:1302–1322
Schofield P (1973) Computer simulation studies of the liquid state. Comput Phys Commun 5:17–23
Scott WRP, Hunenberger PH, Tironi IG et al (1999) The GROMOS biomolecular simulation program package. J Phys Chem A 103:3596–3607
Senn HM, Thiel W (2007) QM/MM methods for biological systems. Atomistic approaches in modern biology: from quantum chemistry to molecular simulations 268: 173–290
Stevens MJ (2001) Simple simulations of DNA condensation. Biophys J 80:130–139
Sun C, Tang T, Uludag H (2011a) Molecular dynamics simulations of PEI mediated DNA aggregation. Biomacromolecules 12:3698–3707

Sun C, Tang T, Uludag H et al (2011b) Molecular dynamics simulations of DNA/PEI complexes: effect of PEI branching and protonation state. Biophys J 100:2754–2763
Sun C, Tang T, Uludag H (2012a) Molecular dynamics simulations for complexation of DNA with 2 kDa PEI reveal profound effect of PEI architecture on complexation. J Phys Chem B 116:2405–2413
Sun C, Tang T, Uludag H (2012b) Probing the effects of lipid substitution on polycation mediated DNA aggregation: a molecular dynamics simulations study. Biomacromolecules 13:2982–2988
Sun C, Tang T, Uludag H (2013) A molecular dynamics simulation study on the effect of lipid substitution on polyethylenimine mediated siRNA complexation. Biomaterials 34:2822–2833
Swope WC, Andersen HC, Berens PH et al (1982) A computer simulation method for the calculation of equilibrium constants for the formation of physical clusters of molecules: application to small water clusters. J Chem Phys 76:637
Szasz D (1996) Boltzmann's ergodic hypothesis, a conjecture for centuries? Studia Scientiarum Mathematicarum Hungaria 31:299–322
Takada S (2012) Coarse-grained molecular simulations of large biomolecules. Curr Opin Struct Biol 22:130–137
Torrie GM, Valleau JP (1977) Nonphysical sampling distributions in Monte Carlo free-energy estimation: umbrella sampling. J Comput Phys 23:187–199
Tuckerman ME (2010) Statistical mechanics: theory and molecular simulation. Oxford University Press, New York
Vasumathi V, Maiti PK (2010) Complexation of siRNA with dendrimer: a molecular modeling approach. Macromolecules 43:8264–8274
Verlet L (1967) Computer "Experiments" on classical fluids. I. Thermodynamical properties of Lennard-Jones molecules. Phys Rev 159:98–103
Voth GA (2009) Coarse-graining of condensed phase and biomolecular systems. CRC Press/ Taylor and Francis Group, Boca Raton
Voulgarakis NK, Rasmussen KO, Welch PM (2009) Dendrimers as synthetic gene vectors: cell membrane attachment. J Chem Phys 130:155101
Warshel A, Levitt M (1976) Theoretical studies of enzymic reactions: dielectric, electrostatic and steric stabilization of the carbonium ion in the reaction of lysozyme. J Mol Biol 103:227–249
Warshel A, Sharma P, Kato M et al (2006) Electrostatic basis for enzyme catalysis. Chem Rev 106:3210–3235
Wereszczynski J, McCammon JA (2012) Statistical mechanics and molecular dynamics in evaluating thermodynamic properties of biomolecular recognition. Q Rev Biophys 45:1–25
Yoon CS, Park JH (2010) Ultrasound-mediated gene delivery. Expert Opin Drug Deliv 7:321–330
Zhang XX, McIntosh TJ, Grinstaff MW (2012) Functional lipids and lipoplexes for improved gene delivery. Biochimie 94:42–58
Zheng M, Pavan GM, Neeb M et al (2012) Targeting the blind spot of polycationic nanocarrier-based siRNA delivery. ACS Nano 6:9447–9454
Ziebarth J, Wang Y (2009) Molecular dynamics simulations of DNA-polycation complex formation. Biophys J 97:1971–1983
Ziebarth J, Wang Y (2010) Coarse-grained molecular dynamics simulations of DNA condensation by block copolymer and formation of core-corona structures. J Phys Chem B 114:6225–6232